# AMP Aptamer Programs DNA Tile Cohesion without Canonical Base Pairing

Zhe Zhang[1], Jin Jin[1], Victoria E. Paluzzi[2], Zhuoer Jin[1], Yuandong Wen[1], Cheng Zhi Huang, Chun Mei Li[1,*], Chengde Mao[1,2,*], Hua Zuo[1*]

[1]Key Laboratory of Luminescence Analysis and Molecular Sensing (Southwest University), Ministry of Education, College of Pharmaceutical Sciences, Southwest University, Chongqing 400715, China

[2]Department of Chemistry, Purdue University, West Lafayette, IN 47907, USA

**ABSTRACT:** Tile-based DNA self-assembly provides a versatile approach for construction of a wide range of nanostructures for various applications such as nanomedicine and advanced materials. The inter-tile interactions are primarily programmed by base pairing, particularly Watson-Crick base pairing. To further expand the tool box for DNA nanotechnology, herein, we have designed DNA tiles to contain both ligands and aptamers. Upon ligand-aptamer binding, tiles associate into geometrically well-defined nanostructures. This strategy has been demonstrated by assembly of a series of DNA nanostructures, which have been thoroughly characterized by gel electrophoresis and atomic force microscopy. This new inter-tile cohesion could bring new potentials to DNA self-assembly in the future. For example, addition of free ligand could modulate the nanostructure formation. In the case of biological ligands, the DNA self-assembly could be related to the presence of certain ligands.

Programmed DNA self-assembly has been extensively studied as a model system of molecular self-assembly.[1, 2] The resulting nanostructures provide potential applications in nanomedicine,[3-6] advanced materials,[7-10] computation,[11, 12] biosensing,[13-14] nanomachines etc.[15-17] The key for DNA self-assembly is DNA base-pairing, Watson-Crick or Non-Watson-Crick (such as G-quadruplex,[18] i-motifs,[19] and triplexes).[20, 21] To further expand the tool box for DNA self-assembly and, more importantly, to introduce non-nucleic acid ligands into the assembly systems, a wide range of interactions have been explored, including metal-base interaction,[22-23] base analogs (e.g. cyanuric acid-adenosine interaction and melamine-thymine interactions),[24-25] and hydrophobic moieties interactions.[26,27] Among them, ligand-aptamer interactions have been explored as a tool for modulate DNA self-assembly,[28-30] but not explicitly as a cohesion force between nanomotifs in well-defined DNA nanostructures. Herein, we report a study that uses the AMP-binding DNA aptamer – adenosine interaction to associate DNA nanomotifs into geometrically well-defined nanostructures. In such a cohesion, no canonical base pairing was involved. This unique study exemplifies a potential way to utilize aptamers in programmed nucleic acid self-assembly.

AMP aptamer is one of the earliest reported DNA aptamers and has been extensively studied.[31-37] It can bind to adenosine and its various phosphate derivatives (AMP, ADP, and ATP) with similar affinities (Kd ~ 10 μM).[35] As shown in an NMR study (Fig. 1a),[32] the aptamer binds to two AMP molecules simultaneously at its 4-nucleotide (nt)-long internal loop (highlighted yellow). The AMP-aptamer complex folds into a duplex structure; wherein the two AMP molecules are located on the same side of the duplex. For the AMP molecule, the base (adenine) and the deoxyribose are buried in the aptamer binding pocket, but the phosphate faces outward and has no contact with the aptamer. Attaching chemicals on the phosphate of the AMP does not affect the aptamer binding.[31] Based on this structural information, we hypothesize that an exposed, unstructured base A at the end of a DNA molecule could bind to the aptamer and such binding could be used as intermolecular cohesion to program DNA self-assembly. This hypothesis was experimentally proven by self-assembly of linear chains, discrete oligomers, and extended two-dimensional (2D) arrays. The assembly structures were thoroughly characterized by native polyacrylamide gel electrophoresis (nPAGE) and atomic force microscopy (AFM).

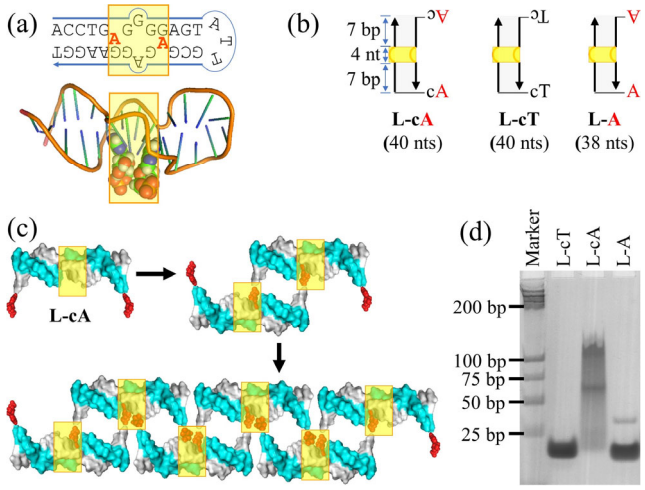


**Figure 1.** AMP-aptamer binding programs the assembly of DNA linear chains. (a) AMP-aptamer complex: sequence and 3D structure. A 4-nucleotide (nt)-long, internal loop is highlighted yellow. AMPs are shown in spheres. (b) Schemes of three, DNA duplex motifs. All contain the AMP-aptamer moiety and the 4-nt-long internal loops (highlighted yellow), but have different overhangs. (c) L-cA motifs self-associate into linear chains by AMP-aptamer binding. The base-As involved in aptamer binding written red or shown as red sphere models. (d) 6% native polyacrylamide gel electrophoresis (nPAGE) analysis of the assembly of DNA linear chains at 4 °C.

We started the exploration by assembly of linear chains from a two-stranded, duplex motif L-cA (Fig. 1). The internal loop of the motif is the AMP aptamer sequence (Figs. 1b and S1). A two-nucleotide (nt)-long overhang, Ac, is included at the 5' end of each strand. The base A is designed

to bind to the aptamer. The extra base, c (cytosine), is added as a spacer to ensure base A has sufficient structural flexibility to bind to the aptamer. The base c is written in lower case to make it clear that it serves as a spacer. The length of the duplex motif was chosen to arrange the two overhangs to be on the side of the duplex that aligned with the binding region (Fig. 1c). Upon A-aptamer binding, the L-cA motifs will associate into linear chains. Between any two associating, adjacent motifs, there will be two, mutual, A-aptamer bindings: one A-base of one motif will bind to the aptamer of the other motif. To test this design, we analyzed the DNA samples by nPAGE (Fig. 1d). The DNA sample appeared as a continuous smear. The L-cA motif contained 40 nts, however the sample migrated much slower than the expected individual motif, which indicated the L-cA motifs associated into large complexes. The continuous smear suggested that the complexes were not uniform in size and they partially dissociated during electrophoresis. To confirm that the large complex formation was indeed due to the A-aptamer binding, we prepared two control motifs, L-cT and L-A, which contained overhangs, Tc or A, respectively. Both motifs contained the aptamer sequence. In motif L-cT, the flexible base A in the overhang was replaced with base T. Thus, motif L-cT did not contain the flexible base A necessary to bind to the aptamer and did not associate into large complexes. In motif L-A, there was no spacer between the duplex and base A. Thus, the base A in motif L-A had reduced flexibility and did not efficiently bind to the aptamer; thus, motif L-A could not effectively associate into large complexes. The experimental data were fully consistent with this reasoning. Motif L-cT appeared as a sharp band with expected mobility for the individual motif (40 nts or ~ 20 bps) and motif L-A dominantly appeared as an individual motif (40 nts or ~ 20 bps) with a very minor population of two interacting motifs (76 nts or ~ 38 bps).

The monovalent, inter-motif interaction for the L-cA motif appeared weak. To address this issue, we applied the concept of bivalent interactions and designed another motif, S-cA, to assemble into a square; a discrete oligomeric complex (Figs. 2, S2, S3). The motif is a single-component hairpin, containing the aptamer internal loop within the duplex stem and two 2-nt-long overhangs (Ac- and -cA) at its 5' and 3' ends, respectively (Fig. 2a). Two A bases of one S-cA motif can simultaneously bind to the aptamer moiety of another motif. Such a bivalent binding is expected to have enhanced stability. Meanwhile the bivalent binding limited the angle between two motifs to near 90° angle. Thus, four S-cA motifs will associate with each other into a homo-tetramer, or a square. Indeed, in the nPAGE, S-cA exhibited a mobility corresponding to a tetramer of an apparent size of ~ 108 bp compared to the individual S-cA motif corresponding to ~ 27 bps (Fig. 2c). A weak dimer band (corresponding to ~ 54 bps) was also observed. The tetrameric structure of the sample was further confirmed by AFM imaging (Fig. 2d).

To confirm that the assembly is due to the A-aptamer binding, we prepared three control motifs (Fig. 2b). (i) S-A. There is no spacer between base A and the duplex region. Due to the reduced flexibility, the A bases should be unable to bind to the aptamer tightly thus, the complex would not be very stable. As a result, a smear corresponding to low molecular sizes was expected. This was confirmed by the nPAGE. (ii) S-c. The motif has no base A in the overhang to bind to aptamer, thus, could not interact with each other at all. (iii) S'-cA. The aptamer moiety was absent in this motif, so no inter-motif interactions were expected. Thus, the mobilities of both S-c and S'-cA motifs corresponded to individual motifs (~24 bps) in the nPAGE. These control experiments confirm that A-aptamer interactions are responsible for the assembly of motif S-cA. We have also found that addition of 2 mM of free adenosine did not significantly change the assembly of S-A compared to S-cA, which suggested that the bivalent A-aptamer binding was much stronger than monovalent adenosine-aptamer binding (Fig. S3). (iv) S-ncA (n = 2, 3, 4). "n" indicates the number of cytosine. The spacer between base A and the duplex contains 2, 3 and 4 cytosine. The flexibility increased when the number of cytosine increased. The motifs tended to associate into larger oligomers, corresponding to the bands with slower mobility in nPAGE (Fig. S2c). (v) S-cA1 and S-cA2. Both motifs have only single binding site. These monovalent A-aptamers did not interact with each other and self-assemble. As such, only separate single bands corresponding to the aptamers were observed in the nPAGE (Fig S2d).

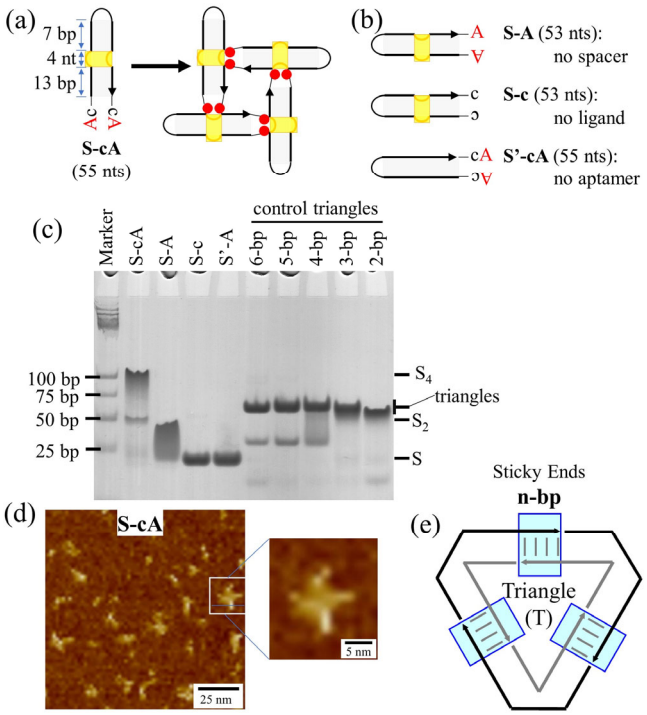


**Figure 2.** Self-assembly of a DNA square. (a) Molecular design of the homo-tetramer assembly. (b) Three control molecules. (c) nPAGE (6%) analysis of the assembly at 4 °C. (d) An AFM image of the complexes assembled from S-cA and a close-up view of an individual complex. (e) Design of control triangles assembled by cohesion of different-length sticky ends (highlighted blue).

DNA self-assembly in most cases is driven by sticky-end cohesion.[1,2] In order to integrate the bivalent A-aptamer interaction into the conventional, sticky-end cohesion-dominated DNA self-assembly systems, it is necessary to calibrate the strength of the bivalent A-aptamer interaction

with that of sticky-end cohesion. For this purpose, we prepared a series of triangles assembled by cohesion of sticky ends with different lengths, and then compared their stabilities with that of the S-cA tetramer by nPAGE (Figs. 2c, 2e and S2a). The control triangle is a design that is the most similar homo-oligomeric complex that we can imagine. Though it is still different from the aptamer-based oligomer, it gives us a rough idea for the binding strength. It appeared that the bivalent A-aptamer interaction was comparable with the cohesion of the 2-bp sticky ends in terms of stability. In both cases, the homo-oligomers formed, but they were not very stable and partially dissociated during electrophoresis, resulting in smears below the main oligomer bands. The aptamer binding is stable at 4 °C (Fig. 2c), but not stable at 25 °C (Fig. S2a). Measuring the binding stability by determining such a low melting temperature (Tm) via UV-visible spectroscopy is experimentally challenging. Thus, we used nPAGE instead.

Even more impressively, the aptamer binding can program DNA motifs to assemble into regular 2D arrays, which exhibited well-defined geometrical arrangement as imaged by AFM (Figs. 3 and S4). Two similar, two-stranded, DNA motifs (2D-a and 2D-b) were designed (Figs. 3a1 and 3b1). Each is a duplex containing: (1) an aptamer internal loop, (2) two, base A-containing overhangs on the end of the left helical domain, and (3) a self-complementary, 4-nt-long, sticky end on the right helical domain. However, the length of the right helical domain is different for the two motifs. The motifs can assemble into squares by the bivalent A-aptamer interaction in the similar fashion for motif S-cA (Figs. 3a2 and 3b2). The squares can further associate via sticky-end cohesion into extended 2D arrays (Figs. 3a3 and 3b3). For 2D-a, the inter-square distance is 26 bps or 2.5 helical turns long (note that the twist of each internal loop is roughly equivalent to 2 bps);[32] thus, any two adjacent squares will face opposite sides of the 2D array plane, eventually leading to corrugated 2D arrays. For 2D-b, the inter-square distance is 32 bps or 3 helical turns long, thus, any two adjacent squares will face the same side of the 2D array plane, eventually leading to non-corrugated 2D arrays. The patterns for the 2D arrays from the two motifs are dramatically different, which were demonstrated by AFM imaging (Figs. 3a4, 3a5, 3b4, and 3b5). We also prepared a series of molecules to confirm that all the three components mentioned above are essential for the 2D array assembly (Fig. S5).

To further demonstrate the aptamer-ligand binding driven DNA self-assembly, we incorporated the aptamer of adenosine (ADE) and investigated the self-assembly behaviors. A motif, S1-cA, derived from the ADE aptamer (G10T-A23),[35] was designed. S1-cA contained overhangs (Ac) and could associate into dimer and trimer, smearing in nPAGE (Fig. S6). As contrast, the controls (S1-c and S1-A) could not self-assemble into complexes.

In conclusion, we have developed a strategy to use aptamer-ligand binding to program DNA self-assembly. It is unique as the aptamer-ligand bond does not involve normal DNA base pairing. This study introduces at least two interesting/useful aspects. (1) It adds a new tool to structural DNA nanotechnology and greatly expands the range of cohesion forces to associate DNA tiles as a great

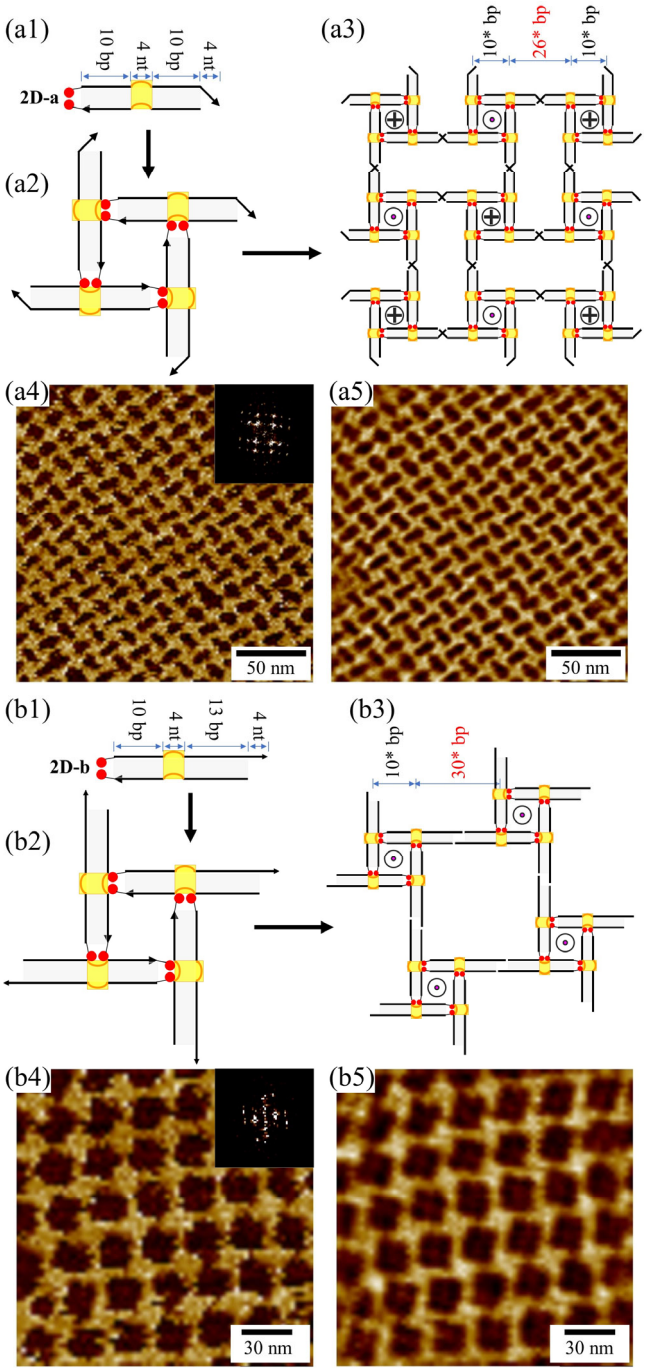


**Figure 3.** Self-assembly of DNA 2D arrays. In the arrays, two adjacent, associating squares face (a) the opposite directions or (b) the same direction. (a1) & (b1): motif design; (a2) & (b2): homo-tetrameric square formed by bivalent A-aptamer binding; (a3) & (b3): sticky-end cohesion allows the motifs to associate by the right helical domains. Dots and crosses in circles indicate the squares facing in and out of the paper plane, respectively. (a4) & (b4): raw AFM images. FFT patterns of the AFM images are included as insets. (a5) & (b5): 2D patterns reconstructed from the corresponding FFT patterns.

number of aptamers are available.[38] (2) It potentially provides a straightforward approach to use various ligands to regulate DNA self-assembly; or, the DNA self-assembly could be responsive to various ligands. As aptamers can be

evolved to recognize many ligands,[38] DNA self-assembly, in principle, can be engineered to be responsive to a wide range of ligands. This will be particularly useful for biosensing and engineering dynamic, biomimetic systems. This strategy should be easily adapted to certain aptamers that recognize natural bases, such as guanosine-binding DNA aptamers and ATP-binding RNA aptamers.[39-40] It is also possible to extend this strategy to aptamers that recognize non-DNA/RNA ligands if the ligands can conjugate to DNAs. However, it is important to note that the molecular design of this strategy is based on the detailed structural information of aptamer-ligand complexes. This strategy will clearly benefit from the large body of structural information of aptamers and the rapid development of structural biology tools such as cryoEM and molecular modeling.

## ASSOCIATED CONTENT

**Supporting Information**. Materials, detailed experimental methods, and additional figures for structural characterization.

## AUTHOR INFORMATION


### Corresponding Authors

***Chun Mei Li** – Key Laboratory of Luminescence Analysis and Molecular Sensing (Southwest University), Ministry of Education, College of Pharmaceutical Sciences, Southwest University, Chongqing 400715, China; orcid.org/0000-0002-3168-2900; Email: licm1024@swu.edu.cn

***Chengde Mao** – Department of Chemistry, Purdue University, West Lafayette, Indiana 47907, United States; orcid.org/0000-0001-7516-8666; Email: mao@purdue.edu

***Hua Zuo** – Key Laboratory of Luminescence Analysis and Molecular Sensing (Southwest University), Ministry of Education, College of Pharmaceutical Sciences, Southwest University, Chongqing 400715, China; orcid.org/0000-0002-8461-8988; Email: zuohua@swu.edu.cn

### Authors

**Zhe Zhang** – Key Laboratory of Luminescence Analysis and Molecular Sensing (Southwest University), Ministry of Education, College of Pharmaceutical Sciences, Southwest University, Chongqing 400715, China; orcid.org/0000-0001-7465-163X

**Jin Jin** – Key Laboratory of Luminescence Analysis and Molecular Sensing (Southwest University), Ministry of Education, College of Pharmaceutical Sciences, Southwest University, Chongqing 400715, China; orcid.org/0009-0000-4412-1128

**Victoria E. Paluzzi** – Department of Chemistry, Purdue University, West Lafayette, Indiana 47907, United States; orcid.org/0009-0004-4397-438X

**Zhuoer Jin** – Key Laboratory of Luminescence Analysis and Molecular Sensing (Southwest University), Ministry of Education, College of Pharmaceutical Sciences, Southwest University, Chongqing 400715, China; orcid.org/0009-0008-3941-3749

**Yuandong Wen** – Key Laboratory of Luminescence Analysis and Molecular Sensing (Southwest University), Ministry of Education, College of Pharmaceutical Sciences, Southwest University, Chongqing 400715, China; orcid.org/0009-0008-9278-2180

**Cheng Zhi Huang** – Key Laboratory of Luminescence Analysis and Molecular Sensing (Southwest University), Ministry of Education, College of Pharmaceutical Sciences, Southwest University, Chongqing 400715, China; orcid.org/0000-0002-1260-5934


### Notes

The authors declare no competing financial interest.

## ACKNOWLEDGMENT


This work was financially supported by the National Science Foundation of China (22134005, 21974111 and 22274135), the Chongqing Research Program of Basic Research and Frontier Technology, China (cstc2021jcyj-msxmX0931, cstc2021jcyj-msxmX1033, and cstc2020jcyj-msxm X0947), Chongqing Talents Program for Outstanding Scientists (cstc2021ycjh-bgzxm0178), and the Applied Basic Research Programs of Science and Technology Department of Sichuan Province, China (2022NSFSC0682). It is also supported by NSF (CCF-2107393 and CCMI-2025187) to C.M.


## REFERENCES


1. Nadrian C. Seeman and Hanadi F. Sleiman. DNA nanotechnology. *Nat. Rev. Mater.* **3**, 17068 (2018).
2. Andre V. Pinheiro, Dongran Han, William M. Shih and Hao Yan. Challenges and opportunities for structural DNA nanotechnology. *Nat. Nanotechnol.* **6**, 763–772 (2011).
3. Qinqin Hu, Hua Li, Lihua Wang, Hongzhou Gu and Chunhai Fan. DNA nanotechnology-enabled drug delivery systems. *Chem. Rev.* **119**, 6459–6506 (2019).
4. Paul S. Kwon, Shaokang Ren, Seok-Joon Kwon, Megan E. Kizer, Lili Kuo, Mo Xie, Dan Zhu, Feng Zhou, Fuming Zhang, Domyoung Kim, Keith Fraser, Laura D. Kramer, Nadrian C. Seeman, Jonathan S. Dordick, Robert J. Linhardt, Jie Chao and Xing Wang. Designer DNA architecture offers precise and multivalent spatial pattern-recognition for viral sensing and inhibition. *Nat. Chem.* **12**, 26–35 (2020).
5. Suping Li, Qiao Jiang, Shaoli Liu, Yinlong Zhang, Yanhua Tian, Chen Song, Jing Wang, Yiguo Zou, Gregory J. Anderson, Jing-Yan Han, Yung Chang, Yan Liu, Chen Zhang, Liang Chen, Guangbiao Zhou, Guangjun Nie, Hao Yan, Baoquan Ding and Yuliang Zhao. A DNA nanorobot functions as a cancer therapeutic in response to a molecular trigger in vivo. *Nat. Biotechnol.* **36**, 258–264 (2018).
6. Jigang Lv, Yuhang Dong, Zi Gu, and Dayong Yang. Programmable DNA nanoflowers for biosensing, bioimaging, and therapeutics. *Chem. Eur. J.* **26**, 14512–14524 (2020).
7. Matthew R. Jones, Nadrian C. Seeman and Chad A. Mirkin. Programmable materials and the nature of the DNA bond. *Science* **347**, 1260901 (2015).
8. Na Liu and Tim Liedl. DNA-assembled advanced plasmonic architectures. *Chem. Rev.* **118**, 3032–3053 (2018).
9. Shawn J. Tan, Michael J. Campolongo, Dan Luo and Wenlong Cheng. Building plasmonic nanostructures with DNA. *Nat. Nanotechnol.* **6**, 268–276 (2011).
10. Yonggang Ke, Luvena L. Ong, William M. Shih and Peng Yin. Three-dimensional structures self-assembled from DNA bricks. *Science* **338**, 1177–1183 (2012).
11. Anna P. Lapteva, Namita Sarraf and Lulu Qian. DNA strand-displacement temporal logic circuits. *J. Am. Chem. Soc.* **144**, 12443–12449 (2022).
12. Damien Woods, David Doty, Cameron Myhrvold, Joy Hui, Felix Zhou, Peng Yin and Erik Winfree. Diverse and robust molecular algorithms using reprogrammable DNA self-assembly. *Nature* **567**, 366–372 (2019).

13. Hong-Min Meng, Hui Liu, Hailan Kuai, Ruizi Peng, Liuting Mo and Xiao-Bing Zhang. Aptamer-integrated DNA nanostructures for biosensing, bioimaging and cancer therapy. *Chem. Soc. Rev.* **45**, 2583–2602 (2016).

14. Xin Chai, Zetan Fan, Ming-Ming Yu, Jian Zhao, and Lele Li. A redox-activatable DNA nanodevice for spatially-selective, AND-gated imaging of ATP and glutathione in mitochondria. *Nano Lett.* **21**, 10047–10053 (2021).

15. Jonathan Bath and Andrew J. Turberfield. DNA nanomachines. *Nat. Nanotechnol.* **2**, 275–284 (2007).

16. Souvik Modi, Swetha M. G., Debanjan Goswami, Gagan D. Gupta, Satyajit Mayor and Yamuna Krishnan. A DNA nanomachine that maps spatial and temporal pH changes inside living cells. *Nat. Nanotechnol.* **4**, 325–330 (2009).

17. Anna-Katharina Pumm, Wouter Engelen, Enzo Kopperger, Jonas Isensee, Matthias Vogt, Viktorija Kozina, Massimo Kube, Maximilian N. Honemann, Eva Bertosin, Martin Langecker, Ramin Golestanian, Friedrich C. Simmel and Hendrik Dietz. A DNA origami rotary ratchet motor. *Nature* **607**, 492–498 (2022).

18. Enjun Cheng, Yongzheng Xing, Ping Chen, Yang Yang, Yawei Sun, Dejian Zhou, Lijin Xu, Qinghua Fan and Dongsheng Liu. A pH-triggered, fast-responding DNA hydrogel. *Angew. Chem. Int. Ed.* **48**, 7660–7663 (2009).

19. Fiona Yutong Huang, Prince Kumar Lat and Dipankar Sen. Unusual paradigm for DNA-DNA recognition and binding:"socket-plug" complementarity. *J. Am. Chem. Soc.* **145**, 3146–3157 (2023).

20. Andrea Idili, Alexis Vallée-Bélisle and Francesco Ricci. Programmable pH-triggered DNA nanoswitches. *J. Am. Chem. Soc.* **136**, 5836–5839 (2014).

21. Yuwei Hu, Alessandro Cecconello, Andrea Idili, Francesco Ricci and Itamar Willner. Triplex DNA nanostructures: from basic properties to applications. *Angew. Chem. Int. Ed.* **56**, 15210–15233 (2017).

22. Guido H. Clever, Corinna Kaul and Thomas Carell. DNA-metal base pairs. *Angew. Chem. Int. Ed.* **46**, 6226–6236 (2007).

23. Simon Vecchioni, Brandon Lu, William Livernois, Yoel P. Ohayon, Jesse B. Yoder, Chu-Fan Yang, Karol Woloszyn, William Bernfeld, M. P. Anantram, James W. Canary, Wayne A. Hendrickson, Lynn J. Rothschild, Chengde Mao, Shalom J. Wind, Nadrian C. Seeman and Ruojie Sha. Metal-mediated DNA nanotechnology in 3D: structural library by templated diffraction. *Adv. Mater.* e2210938 (2023).

24. Qian Li, Jiemin Zhao, Longfei Liu, Sagun Jonchhe, Felix J. Rizzuto, Shankar Mandal, Huawei He, Sansen Wei, Hanadi F. Sleiman, Hanbin Mao and Chengde Mao. A poly(thymine)-melamine duplex for the assembly of DNA nanomaterials. *Nat. Mater.* **19**, 1012–1018 (2020).

25. Nicole Avakyan, Andrea A. Greschner, Faisal Aldaye, Christopher J. Serpell, Violeta Toader, Anne Petitjean and Hanadi F. Sleiman. Reprogramming the assembly of unmodified DNA with a small molecule. *Nat. Chem.* **8**, 368–376 (2016).

26. Jin Liu, Liman Chen, Tingting Zhai, Wei Li, Yuehua Liu and Hongzhou Gu. Programmable assembly of amphiphilic DNA through controlled cholesterol stacking. *J. Am. Chem. Soc.* **144**, 16598–16603 (2022).

27. Ryan A. Brady, Nicholas J. Brooks, Vito Foderà, Pietro Cicuta and Lorenzo Di Michele. Amphiphilic-DNA platform for the design of crystalline frameworks with programmable structure and functionality. *J. Am. Chem. Soc.* **140**, 15384–15392 (2018).

28. Razvan Nutiu and Yingfu Li, Structure-switching signaling aptamers. *J. Am. Chem. Soc.* **125**, 4771–4778 (2003).

29. Juewen Liu and Yi Lu. Fast colorimetric sensing of adenosine and cocaine based on a general sensor design involving aptamers and nanoparticles. *Angew. Chem. Int. Ed.* **45**, 90–94 (2005).

30. Qian Li, Longfei Liu, Dake Mao, Yuyan Yu, Weili Li, Xinfeng Zhao and Chengde Mao. ATP-triggered, allosteric self-assembly of DNA nanostructures. *J. Am. Chem. Soc.* **142**, 665–668 (2020).

31. David E. Huizenga and Jack W. Szostak. A DNA aptamer that binds adenosine and ATP. *Biochemistry* **34**, 656–665 (1995).

32. Chin H. Lin and Dinshaw J. Patel. Structural basis of DNA folding and recognition in an AMP-DNA aptamer complex: distinct architectures but common recognition motifs for DNA and RNA aptamers complexed to AMP. *Chem. Biol.* **4**, 817–832 (1997).

33. Jie Deng and Andreas Walther. ATP-responsive and ATP-fueled self-assembling systems and materials. *Adv. Mater.* **32**, 2002629 (2020).

34. Juewen Liu, Zehui Cao and Yi Lu. Functional nucleic acid sensors. *Chem. Rev.* **109**, 1948–1998 (2009).

35. Juan Canoura, Haixiang Yu, Obtin Alkhamis, Daniel Roncancio, Rifat Farhana and Yi Xiao. Accelerating Post-SELEX aptamer engineering using exonuclease digestion. *J. Am. Chem. Soc.* **143,** 805–816 (2021).

36. Yonatan Biniuri, Bauke Albada and Itamar Willner. Probing ATP/ATP-aptamer or ATP-aptamer mutant complexes by microscale thermophoresis and molecular dynamics simulations: discovery of an ATP-aptamer sequence of superior binding properties. *J. Phys. Chem. B* **122**, 9102-9109 (2018).

37. Zijie Zhang, Olatunji Oni and Juewen Liu. New insights into a classic aptamer: binding sites, cooperativity and more sensitive adenosine detection. *Nucleic Acids Res.* **45**, 7593–7601 (2017).

38. Matthew R. Dunn, Randi M. Jimenez and John C. Chaput. Analysis of aptamer discovery and technology. *Nat. Rev. Chem.* **1**, 0076 (2017).

39. Yuqing Li and Juewen Liu. Highly specific recognition of guanosine using engineered base-excised aptamers. *Chem. Eur. J.* **26**, 13644–13651 (2020).

40. Mandana Sassanfar and Jack W. Szostak. An RNA motif that binds ATP. *Nature* **364**, 550–553 (1993).

**TOC Graphic**